OFFICE OF NAVAL RESEARCH

CONTRACT NO. N00014-86-K-0772

TECHNICAL REPORT NO. 37

"PROCESSING OF THERMOTROPIC LIQUID CRYSTALLINE POLYMERS & THEIR BLENDS"

BY

WAN-CHUNG LEE, ANTHONY T. DIBENEDETTO, AND JACK M. GROMEK

LIQUID CRYSTALLINE POLYMER RESEARCH CENTER
UNIVERSITY OF CONNECTICUT
STORRS, CT 06269-3136

PREPARED FOR PUBLICATION

IN

JOURNAL OF APPLIED POLYMER SCIENCE

FEBRUARY 23, 1990

Unclassified

SECURITY CLASSIFICATION OF THIS PAGE

REPORT DOCUMENTATION PAGE

1a REPORT SECURITY CLASSIFICATION: Unclassified	1b RESTRICTIVE MARKINGS: None
2a SECURITY CLASSIFICATION AUTHORITY	3 DISTRIBUTION/AVAILABILITY OF REPORT: Approved for Public Release, Distribution Unlimited
2b DECLASSIFICATION/DOWNGRADING SCHEDULE	
4 PERFORMING ORGANIZATION REPORT NUMBER(S): Technical Report No.37	5. MONITORING ORGANIZATION REPORT NUMBER(S)
6a. NAME OF PERFORMING ORGANIZATION: University of Connecticut; 6b. OFFICE SYMBOL (If applicable)	7a NAME OF MONITORING ORGANIZATION: Office of Naval Research
6c. ADDRESS (City, State, and ZIP Code): Storrs, CT 06268	7b ADDRESS (City, State, and ZIP Code): 800 North Quincy Avenue Arlington, VA 22217
8a. NAME OF FUNDING/SPONSORING ORGANIZATION: Office of Naval Research; 8b OFFICE SYMBOL (If applicable): ONR	9 PROCUREMENT INSTRUMENT IDENTIFICATION NUMBER: N00014-86-K-0772
8c. ADDRESS (City, State, and ZIP Code): 800 North Quincy Avenue Arlington, VA 22217	10 SOURCE OF FUNDING NUMBERS: PROGRAM ELEMENT NO. / PROJECT NO. / TASK NO. / WORK UNIT ACCESSION NO

11 TITLE (Include Security Classification)
Processing of Thermotropic Liquid Crystalline Polymers & Their Blends (Unclassified)

12 PERSONAL AUTHOR(S)
Wan-Chung Lee, Anthony T. DiBenedetto, and Jack M. Gromek

13a TYPE OF REPORT	13b TIME COVERED	14 DATE OF REPORT (Year, Month, Day)	15. PAGE COUNT
Interim Technical	FROM _____ TO 2-23-90	1990-2-23	49

16 SUPPLEMENTARY NOTATION
Submitted for Publication in Journal of Applied Polymer Science
(LCPRC Publication No.)

17 COSATI CODES			18 SUBJECT TERMS (Continue on reverse if necessary and identify by block number)
FIELD	GROUP	SUB-GROUP	Liquid Crystalline Polymers

19 ABSTRACT (Continue on reverse if necessary and identify by block number)

Preliminary studies were conducted on the hot-drawing of aromatic copolyester LCP fibers (KU-9211 and KU-9221 from Bayer A. G.) and blends of one of these with an aliphatic containing LCP (PET/PHB60 from Tennessee Eastman). The properties of the hot drawn fibers were characterized by measuring storage moduli, E', and molecular orientation parameters, $\langle S \rangle$, as a function of draw ration. A model was developed to correlate both $\langle S \rangle$ and the E' with draw ratio by taking account of thermal relaxation during the drawing process. Agreement between experimental data and the model was obtained by use of a single dimensionless parameter, α, which depends on the processing conditions. An *in-situ* LCP composite of KU-9211 and PET/PHB60 was generated by a combination of blending and hot-drawing and then characterized using SEM, TEM and single-fiber mechanical tests. The dispersed phase consists primarily of highly oriented, 0.5 to 2.0 μm diameter rigid-rods of aromatic fibers imbedded in a matrix of predominantly aliphatic LCP fibrils with diameters in the range of 20 to 50 *n*m. Morphological evidence suggests a strong interfacial adhesion between the dispersed and the matrix phases in this specific system.

20 DISTRIBUTION/AVAILABILITY OF ABSTRACT	21. ABSTRACT SECURITY CLASSIFICATION
☒ UNCLASSIFIED/UNLIMITED ☐ SAME AS RPT ☐ DTIC USERS	Unclassified
22a NAME OF RESPONSIBLE INDIVIDUAL: Dr. Kenneth J. Wynne	22b TELEPHONE (Include Area Code): (202) 696-4410 / 22c. OFFICE SYMBOL: ONR

DD FORM 1473, 84 MAR 83 APR edition may be used until exhausted. All other editions are obsolete

SECURITY CLASSIFICATION OF THIS PAGE
Unclassified

Processing of Thermotropic Liquid Crystalline Polymers & Their Blends

by

Wan-chung Lee, Anthony T. DiBenedetto** and Jack M. Gromek

Department of Chemical Engineering

& Institute of Material Science

The University of Connecticut, Storrs

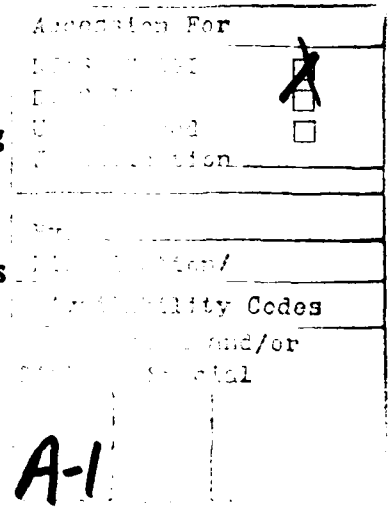

** To whom correspondence should be addressed.

Processing of Thermotropic Liquid Crystalline Polymers & Their Blends

W. Lee, A. T. DiBenedetto and J. M. Gromek

Department of Chemical Engineering & Institute of Material Science

The University of Connecticut, Storrs, CT 06268

Synopsis

Preliminary studies were conducted on the hot-drawing of aromatic copolyester LCP fibers (KU-9211 and KU-9221 from Bayer A. G.) and blends of one of these with an aliphatic containing LCP (PET/PHB60 from Tennessee Eastman). The properties of the hot drawn fibers were characterized by measuring storage moduli, E', and molecular orientation parameters, $<S>$, as a function of draw ratio. A model was developed to correlate both $<S>$ and the E' with draw-ratio by taking account of thermal relaxation during the drawing process. Agreement between experimental data and the model was obtained by use of a single dimensionless parameter, α, which depends on the processing conditions. An 'in-situ' LCP composite of KU-9211 and PET/PHB60 was generated by a combination of blending and hot-drawing and then characterized using SEM, TEM and single-fiber mechanical tests. The dispersed phase consists primarily of highly oriented, 0.5 to 2.0 μm diameter rigid-rods of aromatic fibers imbedded in a matrix of predominantly

aliphatic LCP fibrils with diameters in the range of 20 to 50 *n*m. Morphological evidence suggests a strong interfacial adhesion between the dispersed and the matrix phases in this specific system.

Processing of Thermotropic Liquid Crystalline Polymers & Their Blends

W. Lee, A. T. DiBenedetto and J. M. Gromek
Department of Chemical Engineering & Institute of Material Science
The University of Connecticut, Storrs, CT 06268

INTRODUCTION

The increasing demands for ultrahigh modulus and strength fibers and plastics have drawn a considerable interest in both academe and industry in the field of liquid crystalline polymers (LCPs). The existing lyotropic Kevlar and thermotropic polyester fibers, for example, have been reported to have tensile moduli in the range of 30-120 GPa, depending on both the chemical composition and the processing conditions[1-3] . The specific tensile moduli (stiffness per unit weight) of these LCP fibers are approximately three times higher than those of the steel and glass fibers, and are about ten times of those of the organic fibers such as nylon and PET[1]. It seems that the ease of achieving high modulus and strength of the LCPs is due to the rigid rod-like or plate-like molecular structure of the LCPs forming anisotropic solutions or melts which are potentially capable of producing a high degree of molecular orientation during the processing procedures. The attractive mechanical properties combined with some other optical and physical characteristics have

made these liquid crystalline polymers one of the most promising classes of materials in the applications of the electric/electronic, chemical, transportation and aerospace industries.

In recent years, extensive studies have been focused on thermotropic liquid crystalline polymers. Instead of using solvents for the formation of a mesophase as in the lyotropic system, thermotropic LCPs exhibit mesomorphic melts within a defined temperature range. Through appropriate modifications of the molecular structures such as random copolymerization of moieties having flexible chains, bulk side groups, or kinked linkages, a very broad range of physical properties can be obtained. They are then melt processable with conventional thermoplastic processing techniques, such as injection molding or melt spinning but still retain the liquid crystalline order. Due to rheological characteristics such as relatively lower viscosity, longer relaxation time[3-8] and higher rate of molecular orientation under an elongational flow field (when compared with coventional isotropic polymers at a comparable molecular weight)[9], molded articles of the thermotropic LCPs retain a high degree of molecular anisotropy in the flow direction upon solidification. The resulting mechanical properties are often found equivalent or even superior to those of glass fiber-reinforced polymer composites[1-3].

In addition, these melt-processable thermotropic LCPs are also a prime candidates for reinforcing 'in-situ' traditionally used engineering plastics. The general approach has been to extrude or draw a blend of the LCP in the

molten state with conventional thermoplastics. When the LCP is a minor component, it forms highly elongated fibrous structures parallel to the flow direction during processing. The inherently high strength and stiffness of the LCPs therefore improve the mechanical properties of the resulting blend. A number of research groups[10-22] have been studying the effects of composition on rheology, mechanical properties and the structure of LCP blends with traditional engineering thermoplastics, both crystalline and amorphous, including polycarbonate(PC), polystyrene(PS), poly(ethylene terephthalate) (PET), polyamides (such as nylon 6/6) among others. It seems, however, that the adhesion between phases is poor in most cases, which is critical in determining the mechanical properties of the blends.

In a continuing study we are examining the drawing characteristics of some thermotropic LCPs and their blends with the objective of producing a composite blend of fibers in which the dispersed phase is thermally stable during a subsequent molding operation and the fibrous matrix phase is processable and potentially compatible with both the dispersed phase and a possible third component such as a thermoplastic matrix. Two major aspects of these goals are covered in this preliminary study. One is to investigate the drawing characteristics of two LCPs. With some modification of a composite model previously developed[26], we are able to correlate the mechanical properties with the drawing variables. The other aspect includes both morphological and mechanical studies on the LCP blends in order to investigate the compatibility and adhesion between different fibrous phases.

ANALYSIS OF HOT-DRAWING PROCESS

In a study by Ide and Ophir[9], it was found that neither the orientation nor the filament modulus were dependent on the take-up stress (or elongational stress) in a melt spinning process, but rather were strong functions of the elongational strain (or draw-down ratio). Blizard et al.[23] studied the relationship between the tensile modulus and the draw-down ratio for uniaxially drawn films of Vectra (HBA/HNA from Celanese Co.) and X7G (PET/PHB60 from Tennessee Eastman Co.). They found that there was a definite increase in modulus with the draw-ratio, suggesting that at least a portion of the orientation was retained in the post-extrusion processing. Kenig[24] developed a flow model for extrusion and melt spinning of liquid crystalline polymers based on the rigid-rod rotation analogy, assuming that the experimentally observed 'domains' in the LCPs are the species responsible for the orientation development. It was also concluded that in the elongational flow, the orientation of these rigid species was dependent on the overall elongational deformation (or draw-down ratio) and a material parameter λ. The dependence of the orientation on the draw-down ratio was expressed in the form[24]:

$$\tan \varphi = \tan \varphi_0 (DR^{-\lambda}) \tag{1}$$

where φ is the instaneous orientation angle of a rigid particle makes with the elongation direction, φ_0 is the initial orientation angle and λ is a material parameter which depends on the polymer characteristics. Equation (1) was also

obtained by Nicholais et al.[25] with $\lambda = 3/2$ for short fiber reinforced extruded sheet, assuming that the matrix maintained a constant volume prior to the fiber breakage.

DiBenedetto et al.[26] recently developed a composite model based on the rigid-rod rotation mechanism but also took into consideration the deformation of the domains in the elongational flow field. The relationship between the orientation function of the nematic domains in the fiber, S_N , and the draw-ratio (DR) was derived as:

$$S_N = \frac{(2S_{N0} + 1)(DR)^3 - (1 - S_{N0})}{(2S_{N0} + 1)(DR)^3 + 2(1 - S_{N0})} \tag{2}$$

where S_{N0} is the initial orientation function of these domains upon exiting the extruder. The orientation function is defined by the Herman's orientation function:

$$S = \frac{1}{2}(3 < \cos^2\varphi > - 1) \tag{3}$$

and

$$< \cos^2\varphi > = \frac{\int_0^{\pi} g(\varphi) \cos^2\varphi \sin \varphi d\varphi}{\int_0^{\pi} g(\varphi) \sin \varphi d\varphi} \tag{4}$$

in which φ is the average angle between the directors and the drawing direction, and $g(\varphi)$ is an angular distribution function for the molecular vectors. It can be seen from eqns.(3) and (4) that when the domains are all randomly distributed, the orientation function $S_N = 0$; when they are perfectly aligned along the drawing direction $\varphi = 0$, and $S_N = 1$.

In addition to rotation, the nematic domains can be deformed in an elongational field. It was assumed that in the absence of any external stresses the nematic domains were randomly oriented polyhedra with an average aspect ratio (i.e., length-to-diameter ratio, l/d) of 1. In the presence of an elongational stress field these domains will simultaneously rotate and translate and the aspect ratio of the domains increases as a function of the draw-ratio. Hence, the orientation function of the nematic domains, S_N, would range from 0 when $l/d = 1$ and the domains were randomly oriented to 1 when l/d goes to infinity and the domains were perfectly aligned in the direction of the fiber axis.

The previous work did not take into account the thermally induced relaxation of the oriented and deformed domains during the drawing process. In this study we propose a relaxation model previously used by Ziabicki and Kedzierska[27] to interrelate the molecular orientation and the elastic moduli through a dimensionless processing parameter α.

It is assumed that the rotation and the deformation of the nematic domains are connected in that

$$S_N = 0 \quad \text{when} \quad l/d = 1 \qquad \text{and} \qquad S_N = 1 \quad \text{when} \quad l/d \to \infty$$

We further assume that the rigid rotation and mechanical distortion of the domains are diminished by a single, linear thermal relaxation process, i.e.,

$$\text{Relaxation} \propto \exp(-\tau_R) = \exp(-\theta/\tau) \tag{5}$$

where τ_R is the reduced relaxation time for both orientation and distortion, θ is the time of travel from the exit of the extruder to the take-up device, and τ is the molecular relaxation time. The relaxation time is a complicated function of the processing conditions and is virtually impossible to determine as a function of the variation of temperature and orientation because of the gross changes in morphology occurring in the hot-drawing zone.

Ziabicki and Kedzierska[27] suggested that the mean relaxation time, τ, for the polymer in a melt-spinning process could be substituted by the comparative cooling rate, Z, along the spinning path from 0 to l_E:

$$\tau \propto Z = -\frac{d \ln(T - T_0)}{dl} \tag{6}$$

in which T is the filament temperature along the spinning path l, l_E is the length of the spinning path and T_0 is the temperature of the cooling medium. The analogy between the relaxation time and the cooling rate in the melt-

spinning process can be understood as follows. When the cooling rate is high the drawn fibers will be 'frozen' quickly, thus preventing significant relaxation of the orientation generated during the drawing process. This can be imagined as a process with a long relaxation time. On the other hand, when the cooling of the filament is slow, it tends to remain at a relatively high temperature during the drawing process and relaxation will occur more readily, which is equivalent to saying that the process is characterized by a short relaxation time. The cooling rate parameter Z was estimated from the spinning conditions by the approximation[27]:

$$Z = -\left(\frac{1}{l_E}\right)^* Bi^* Fo \tag{7}$$

in which Bi and Fo are the resulting Biot and Fourier numbers along the drawing path, respectively. Therefore, to a first approximation, the relaxation time τ relates to the cooling condition of the hot-drawing process in the manner of :

$$Z \propto \tau = K^* Bi^* Fo = \frac{4\,K\,h_{ave.}\,\theta}{\rho_f C_{pf} d_f} \tag{8}$$

where

ρ_f = density of the fiber,
C_{pf} = specific heat of the fiber,
d_f = final fiber diameter,
K = proportionality constant,
$h_{ave.}$ = average heat transfer coefficient.

The orientation parameter of the nematic domains (eq. (2)) can thus be re-defined as a function of both the draw-ratio and the relaxation time as:

$$S_N = \frac{(2S_{N0} + 1)(DR)^3 - (1 - S_{N0})}{(2S_{N0} + 1)(DR)^3 + 2(1 - S_{N0})} \exp(-\theta/\tau) \tag{9}$$

and the aspect ratio is assumed to have the form

$$(l/d)_f = \{(l/d)_0 (DR)^{3/2} - 1\} \exp(-\theta/\tau) + 1 \tag{10}$$

where $(l/d)_0$ is an average aspect ratio for the domains at the beginning of the drawing process. Equation (10) satisfies the boundary conditions:

$$(l/d)_f = (l/d)_0 \ (DR)^{3/2} \qquad \text{as} \qquad \tau \to \infty$$

$$(l/d)_f = 1 \qquad \text{as} \qquad \tau \to 0 \tag{11}$$

By employing the empirical heat-transfer equation relating the Nusselt number Nu to a Reynolds number Re suggested by Kase and Matsuo[28] for a stationary rod in axial air stream, $Nu = 0.42\ Re^{0.334}$, the reduced relaxation time, τ_R, can be derived from equation (8) as the ratio of one dimensionless parameter α and the draw ratio:

$$\tau_R = \frac{\theta}{\tau} = \frac{\rho_f C_{pf} d_f}{4\ K\ h_{ave.}}$$

$$= \left(\frac{\rho_f C_{pf} d_0^{\,2}}{1.68\ K\ k_{air}}\right) \left(\frac{v_{air}}{V_0\ d_0}\right)^{0.334} \frac{1}{DR^{1.167}}$$

$$= \frac{\alpha}{DR^{1.167}} \tag{12}$$

in which

d_0 = initial fiber diameter,
k_{air} = thermal conductivity of the cooling air,
v_{air} = kinematic viscosity of the cooling air,
V_0 = initial velocity of the fiber at the exit of extruder, and
DR = draw ratio = $(d_0/d_f)^2$.

Hence, the molecular orientation and the deformation of the molecular domains are related to the draw ratio and other processing conditions by:

$$S_N = \frac{(2S_{N0} + 1)(DR)^3 - (1 - S_{N0})}{(2S_{N0} + 1)(DR)^3 + 2(1 - S_{N0})} \exp\left(-\frac{\alpha}{DR^{1.167}}\right) \tag{13}$$

$$(l/d)_f = 1 + \{(l/d)_0(DR)^{3/2} - 1\} \exp\left(-\frac{\alpha}{DR^{1.167}}\right) \tag{14}$$

The parameter α is a dimensionless quantity which depends on both the conditions at the exit of the extruder and those of the cooling medium. The relation between the moduli of the fiber and the draw ratio is then obtained by applying the well-known Halpin-Tsai equations along with equation (14), as was done previously[26] . The molecular orientation parameter for the fiber, S_F, is defined as:

$$S_F = S_N \; X_N \tag{15}$$

where X_N is an equivalent volume fraction of oriented liquid crystalline domains and can be estimated from WAXS information on the highly drawn fibers. The longitudinal modulus of the fiber is given by the following equation[26] :

$$\frac{E_{LF}}{E_A} = \frac{1 + 2(l/d)_f \; B \; X_N}{1 - BX_N} \tag{16}$$

and

$$B = \frac{(E_N/E_A)_L - 1}{(E_N/E_A)_L + 2 \; (l/d)_f} \tag{17}$$

where E_N is the longitudinal modulus of the perfectly oriented liquid crystalline domains ($S_N = 1$) and E_A is the modulus of the 'non-oriented' portion (i.e., the matrix) of the fiber.

EXPERIMENTAL

The materials used in this study were two LCPs developed by Bayer A. G. under the names of KU-9211(also called K161) and KU-9221(K209). Both materials are obtained from the esterification of aromatic compounds: HA(hydroxybenzoic acid) / HQ(hydroquinone) / TA(terephthalic acid) / HBP(4,4'-hydroxy bisphenol). The structural difference between these two is that K161 uses IA(isophthalic acid) as the kinked structure in the molecules;

whereas K209 uses bisphenol-A to affect the packing between polymer chains. Both have melting points of about 300°C. Also used was the LCP PET/PHB60 (batch number: X19040-88, graciously supplied by the Kodak Tennessee Eastman Co.). Pellets of all LCPs were vacuum dried at 100°C for over 24 hours. Fibers of different draw-ratios were drawn from a CSI Maxwell extruder at 340°C. These fibers were then characterized by using wide angle X-ray (WAXS) analysis and dynamic mechanical tests (DMTA) to determine the orientation parameters and the dynamic moduli of these fibers, respectively.

Digitized diffraction data were collected using a Rigaku RU-200 X-ray generator equipped with a Nicolet area detector and a Buerger Precession Camera (Cu-Kα radiation $\lambda = 1.5418$Å). Following background subtraction and the necessary instrumental corrections, data frames were then transferred through a micro-VAX system to an IBM PC where data manipulation was done using POLYGRAF[29]. The Herman's orientation parameter $<S>$ was then estimated from the azimuthal intensity profile for each fiber at different draw-ratios. Polymer Laboratory's dynamic mechanical-thermal analyzer (DMTA) was used to measure the storage and loss moduli of these fibers at 1 Hz. At room temperature these fibers are in their glassy states so the storage moduli obtained are a good estimation of the tensile moduli.

An LCP blend was prepared by mixing 30 wt% of K161 and 70% of PET/PHB60 in the Brabender at 345°C and 40 rpm for 30 mins. The mixture

was then quenched to the room temperature and fibers of the mixture were then drawn from the CSI Maxwell extruder at 260°C. Characterizations of the blend included dynamic mechanical tests (DMTA), scanning electron microscopy (SEM) as well as transmission electron microscopy (TEM). The stress-strain relationship for pure components as well as the blend was estimated from the single-fiber test following ASTM D3379-75. Single fibers were glued at each end to a cardboard tab with gauge length of 1 inch. The stress-strain curves were then obtained by using an Micro Tensile tester (MTS) at a crosshead speed of 2 inches per minute.

RESULTS AND DISCUSSION

Fig.1 shows typical flat-plate Laue diffraction of K209 fibers at three different draw-ratios (with the fibers in the vertical direction). The overall pattern indicates the nematic character of these LCP fibers[30]. As the draw-ratio increases, the azimuthal spread of the equatorial diffraction pattern becomes sharper, suggesting an increase in molecular orientation. Similar behavior was obtained for K161 fibers. Fig.2 shows the experimental values of the storage moduli and the orientation parameters at different draw-ratios for both K161 and K209 fibers. It can be seen that the orientation parameters for both fibers reach a plateau of $<S> \sim 0.9$ at DR close to 20, whereas the storage moduli data show steady increases over a much wider range of the draw-ratio (DR). The K161 fibers seem to be a little stiffer than the K209 fibers under the cho-

sen processing conditions. Data were fitted with the proposed model (eqns.(13) & (14) along with the Halpin-Tsai equations for calculating the moduli) as also shown in the figure. Best fits of the data were obtained with values for the dimensionless parameter $\alpha = 0.38$ and 0.42 for K161 and K209, respectively. As discussed above, the dimensionless parameter α depends on the physical properties of the fibers as well as the drawing conditions. Since the drawing conditions such as the extrusion rate, melt temperature and the density as well as the heat capacity are similar for both fibers, it is expected that the α values for K161 and K209 should be close to each other as obtained experimentally. Fig.3 shows the relationship between modulus and draw-ratio for PET/PHB60 fibers from a previous experiment[26], also fitted with the model and using a value of the parameter $\alpha = 1.23$. The model appears to fit both the modulus and the orientation parameter simultaneously with only one dimensionless parameter α. With a better control of the drawing conditions, we should be able to predict the mechanical properties of LCP fibers as a function of process conditions. Such a study is presently in progress.

The LCP/LCP blend was prepared following the recipe described in the experimental section. Fig.4 shows the loss tangent of the quenched 30K161/70PET(PHB60) blend along with data for both pure components. K161 shows a single T_g around 135°C and melts at about 300°C (not in the scale of Fig.4). PET/PHB60, on the other hand, has two T_gs at 70 and 110°C and melts around 220°C. The glass transition at around 70°C is attributed to the PET-rich phase, while the other at around 110°C is attributed to

the PHB-rich phase. The quenched blend of K161/PET(PHB60) has only one T_g around 105°C and melts at around 210°C. This result suggests that either the two LCPs are miscible in the melt or, possibly, they have reacted through ester exchange and have formed a new random copolymer. To distinguish between the two possibilities, we annealed the quenched blends at 250°C for different amounts of time and used SEM to study the corresponding morphology. Fig.5 shows the SEM pictures of a series of annealed blends. As can be seen, the unannealed sample is a homogeneous, one-phase mixture (at least on the scale of microns), while the annealed samples all show phase separation. Two close-ups of the interfaces between the two components are shown in Fig.6 for the samples annealed for 4 and 24 hours, respectively. It is thus clear that K161 and PET/PHB60 are miscible in a 30/70 blend above their melt temperatures and only partially miscible, or perhaps immiscible, at lower temperatures. This observation is consistent with the concepts proposed by Jin et al.[31] and investigated by De Meuse & Jaffe[32] . Upon annealing, a dispersed second phase of spheres precipitates, which we think is a K161 or K161-rich phase judging from the volume content. As the annealing time increases, more and more small spheres precipitate and tend to agglomerate (Fig.6 (b)). It is also clear that strong adhesion exists at the interfaces between phases. Although the possibility of transesterification has not been entirely dismissed, there is no clear evidence of chemical reaction. Upon annealing one cannot clearly see a regeneration of the original glass transition temperatures of the individual components, so it is likely that both phases contain two components. The measured volume fractions, the presence of common blocks

of HBA in the two components and the high level of adhesion between phases lends credence to the likelihood that there is partial miscibility of the two components. A phase diagram for this system is yet to be obtained.

Fibers of the 30K161/70PET(PHB60) blend were drawn from a CSI Maxwell extruder at 260°C. Fig.7 shows the cross-section of the fracture surface of the resulting fiber broken in liquid nitrogen. One can see a dispersed brittle phase imbedded in a ductile matrix. From the mechanical properties, the drawing characteristics and the melting temperatures of these two components, it is quite likely that the imbedded phase is either a K161 or a K161-rich phase, and that the matrix is a PET/PHB60 or a PET/PHB60-rich phase. Furthermore, the K161-rich phase having average dimensions about 1μm is strongly bonded to the PET/PHB60 phase which has a fibrillar structure with dimensions of the order of 20 to 50 *n*m. Fig.8 reinforces the observation by showing the longitudinal fracture surfaces of the fibers. As can be seen, the fiber of the LCP blend consists of bundles of fibrils stongly bonded together. Each bundle consists of rigid, brittle fibers surrounded by the ductile 20-50 *n*m fibrils.

Fig.9 is a series of TEM photographs showing the cross-section of the 30K161/70PET(PHB60) fiber. The samples were prepared by microtoming the fiber into thickness around 700Å and staining with uranyl acetate followed by lead citrate. Figure 9-(a) shows the transverse cross-section of the fiber surface in which the black circular-shaped, dispersed domains were identified

as the K161-rich phase. The radial size distribution of the K161-rich phase shows that thermal gradients during drawing play an important role in the hot-drawing process. Around the edges of the fiber, fast cooling occurs during the drawing process and the highly elongated and oriented domains of the precipitated phase are quickly 'frozen'. Toward the center of the fiber these domains relax due to the slower cooling, resulting in numerous domains of larger sizes. Fig.9-(b) is a close-up view of an interface between the two fiber phases. We see a continuous color change over about 50*n*m indicating a continuous material gradient between the dispersed and the matrix phases. Fig.9-(c) is a picture of the longitudinal cross-section. The brittle and ductile fracture characteristics of the two are clearly shown. All of the microscope photographs confirm strong bonding between the two phases.

Table 1 summarizes the mechanical properties of both components, K161 and PET/PHB60, and the blend in 30/70 weight ratio from the single fiber tests. The results were also compared with the calculated values using the rule of mixtures. It is seen that both the Young's modulus and the breaking strength of the blend are approximately equal to, albeit a little lower than, values estimated by the rule of mixtures. The breaking strain is closer to that of the brittle dispersed phase, as expected.

CONCLUSIONS

Two major objectives were achieved in this study: (1) to relate the molecular orientation and elastic properties of the LCP fibers to the variables of a hot-drawing process, and (2) to produce an LCP fiber blend in which the fibrous dispersed phase is thermally stable during subsequent molding operations and the fibrous matrix phase is both processable and potentially compatible with the dispersed phase and a possible third component such as a thermoplastic matrix. With regard to the first objective, a model describing the rotation and deformation of nematic domains, subject to thermal relaxation during hot drawing, appears to describe both the orientation parameter and storage moduli data simultaneously with only one dimensionless parameter α which is a function of process conditions. The two LCPs from Bayer A. G. used in this study achieved a high molecular orientation with $<S> \sim 0.9$ at *DR* around 20. The longitudinal elastic modulus, on the other hand, showed a steady increase with the draw-ratio reaching a plateau in the range of 30 to 50 GPa at draw ratios above 300 to 500. Further study is now being conducted in a well controlled hot-drawing system in which all process conditions can be systematically varied in order to test the dimensional analysis.

With regard to the second objective, an LCP fiber was produced from a 30/70 blend of the aromatic copolyester (K161) and a PET/PHB60 thermotropic LCP. The dispersed (K161-rich) phase was an array of rigid, brittle fibers, with diameters of the order of 1μm, imbedded in a (PET/PHB60-rich) phase which had a fibrillar stucture with diameters of the order of 20 to 50*nm*. The rigid dispersed fiber phase had a thermal stability

to well above the melting point of K161 of about 300°C, while the fibrous matrix appears to be a nematic liquid crystal above 110°C and becomes processable in the temperature range 220 to 260°C. It has been shown that the two phases are strongly bonded. It is envisioned that this concept can be expanded to provide a practical method of developing 'in-situ' coupling between thermally stable, thermotropic fibers and incompatible thermoplastic matrices using the partially compatible and processable LCP as an intermediate phase, in much the same fashion as has been applied to PE-PS and other blends[33-34]. A ternary blend might be expected to have a better mechanical properties than those of most incompatible LCP/thermoplastic pairs if the intermediate coating were either reactive or partially compatible with the other two phases. It is with this goal in mind that we have initiated a program of studying the thermodynamic, rheological and chemical properties of some model ternary systems.

ACKNOWLEDGEMENT

The authors would like to express our gratitude to Dr. H. D. Keith for the discussion of TEM results and to Dr. A. W. Wachtel and his assistant J. S. Romanow of the Biology Department for their constant assistance in the SEM and TEM studies.

REFERENCES

1. G. W. Calundann and M. Jaffe, in *Proceedings of The Robert A. Welch Conference on Chemical Research XXVI*, Synthetic Polymers, Texas, 1982, pp. 247-291.

2. D. C. Prevorsek, in *Polymer Liquid Crystals*, A. Ciferri, W. R. Krigbaum and R. B. Meyer, Eds., Academic Press, New York, 1982, pp. 329-376.

3. Y. Ide and T.-S. Chung, *J. Macromol. Sci.,-Phys.*, **B23**(4-6), 497 (1984-85).

4. K. F. Wissbrun and A. C. Griff, *J. Polym. Sci., Polym. Phys. Ed.*, **20**, 1835 (1982).

5. K. F. Wissbrun, *Brit. Poly. J.*, Dec., 163 (1980).

6. K. F. Wissbrun, *J. Rheol.*, **25**, 619 (1981).

7. E. G. Joseph, G. L. Wilkes and D. G. Baird, *Polym. Eng. Sci.*, **25**, 377 (1985).

8. D. G. Baird, in *Polymeric Liquid Crystals*, A. Blumstein, Ed., Plenum Press, New York, 1985, pp. 119-143.

9. Y. Ide and Z. Ophir, *Polym. Eng. Sci.*, **23**(5), 261 (1983).

10. W. Huh, R. A. Weiss and L. Nicolais, *Polym. Eng. Sci.*, **23**(14), 779 (1983).

11. A. Siegmann, A Dagan and S. Kenig, *Polym.*, **26**, 1325 (1985).

12. E. G. Joseph, G. L. Wilkes and D. G. Baird, in *Polymeric Liquid Crystals*, A. Blumstein, Ed., Plenum Press, New York, 1985, pp. 197-216.

13. A. I. Isayev and M. J. Modic, *SPE ANTEC Tech. Papers*, 573 (1986).

14. T.-S. Chung, *SPE ANTEC Tech. Papers*, 1404 (1987).

15. K. G. Blizard and D. G. Baird, *Polym. Eng. Sci.*, **27**(9), 653 (1987).

16. R. Ramanathan, K. G. Blizard and D. G. Baird, *SPE ANTEC Tech. Papers*, 1399 (1987).

17. G. Kiss, *Polym. Eng. Sci.*, **27**(6), 410 (1987).

18. R. Ramanathan, K. G. Blizard and D. G. Baird, *SPE ANTEC Tech. Papers*, 1123 (1988).

19. P. Zhuang, T. Kyu and J. L. White, *Polym. Eng. Sci.*, **28**(17), 1095 (1988).

20. M. R. Nobile, E. Amendola, L. Nicolais, D. Acierno and C. Carfagna, *Polym. Eng. Sci.*, **29**(4), 244 (1989).

21. W. Brostow, T. S. Dziemianowicz, J. Romanski and W. Werber, *Polym. Eng. Sci.*, **28**(12), 785 (1988).

22. C. U. Ko and G. L. Wilkes, *J. Appl. Polym. Sci.*, **37**, 3063 (1989).

23. K. G. Blizard, D. Done and D. G. Baird, *SPE ANTEC Tech. Papers*, 551 (1988).

24. S. Kenig, *Polym. Eng. Sci.*, **27**(12), 887 (1987).

25. L. Nicolais, L. Nicodemo, P. Masi and A. T. DiBenedetto, *Polym. Eng. Sci.*, **19**(14), 1046 (1979).

26. A. T. DiBenedetto, L. Nicolais, E. Amendola, C. Carfagna and M. R. Nobile, *Polym. Eng. Sci.*, **29**(3), 153 (1989).

27. A. Ziabicki and K. Kedzierska, *J. Appl. Polym. Sci.*, **11**(4), 14 (1959).

28. S. Kase and T. Matsuo, *J. Polym. Sci.*, **A3**, 2541 (1965).

29. J. M. Gromek, Unpublished computer package for digitized data analysis.

30. L. V. Azaroff, *Mol. Cryst. Liq. Cryst.*, **145**, 31 (1987).

31. J.-I. Jin, E.-J. Choi and K.-Y. Lee *Polym. J.*, **18**(1), 99 (1986).

32. M. T. De Meuse and M. Jaffe, *Mol. Cryst. Liq. Cryst. Inc. Nonlin. Opt.*, **157**, 535 (1988).

33. D. R. Pau', J. W. Barlow and H. Keskkula in *Encyclopedia of Polymer Science and Engineering*, H. F. Mark et al., Eds., vol. 12, 2nd ed., Wiley, New York, 1988, p. 399.

34. R. Fayt, R. Jerome and P. Teyssie, in *Multiphase Polymers*, L. A. Utracki and R. A. Weiss, Eds., chap.2, ACS Series 395, 1989, p. 38.

LIST OF TABLES

LIST OF FIGURES

Fig. 1 Wide-angle x-ray diffraction patterns for K209 fibers of DR = (a) 2 (b) 30 (c) 66.

(a)

Fig. 1 Wide-angle x-ray diffraction patterns for K209 fibers of DR = (a) 2 (b) 30 (c) 66.

(b)

(Continued from the previous page.)

Fig. 1 Wide-angle x-ray diffraction patterns for K209 fibers of DR = (a) 2 (b) 30 (c) 66.

(c)

(Continued from the previous page.)

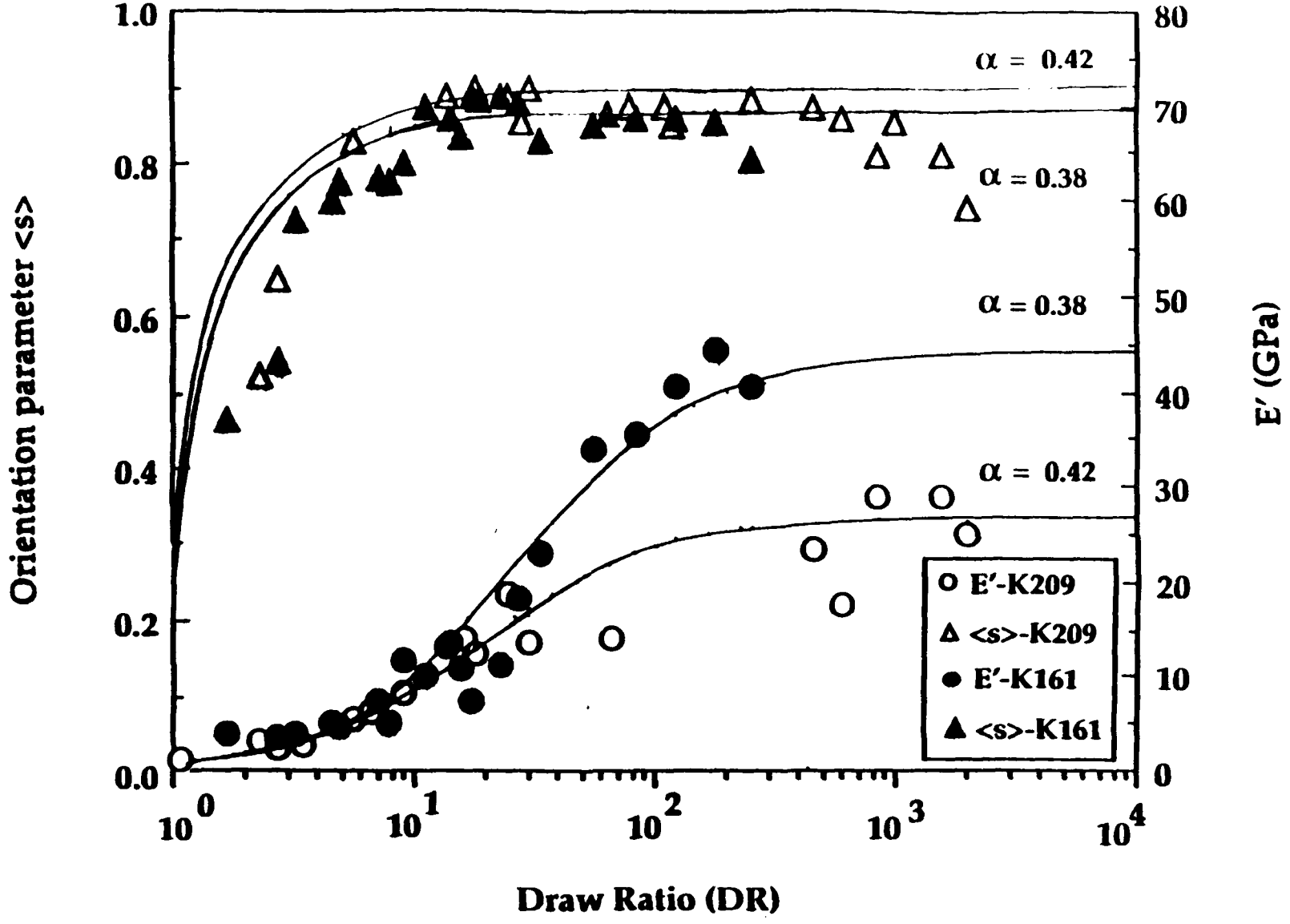

Fig. 2 Experimental data of orientation parameter <S> and the storage modulus E' for both K209 and K161 fibers. Data are fitted with the model with the parameter α value as indicated.

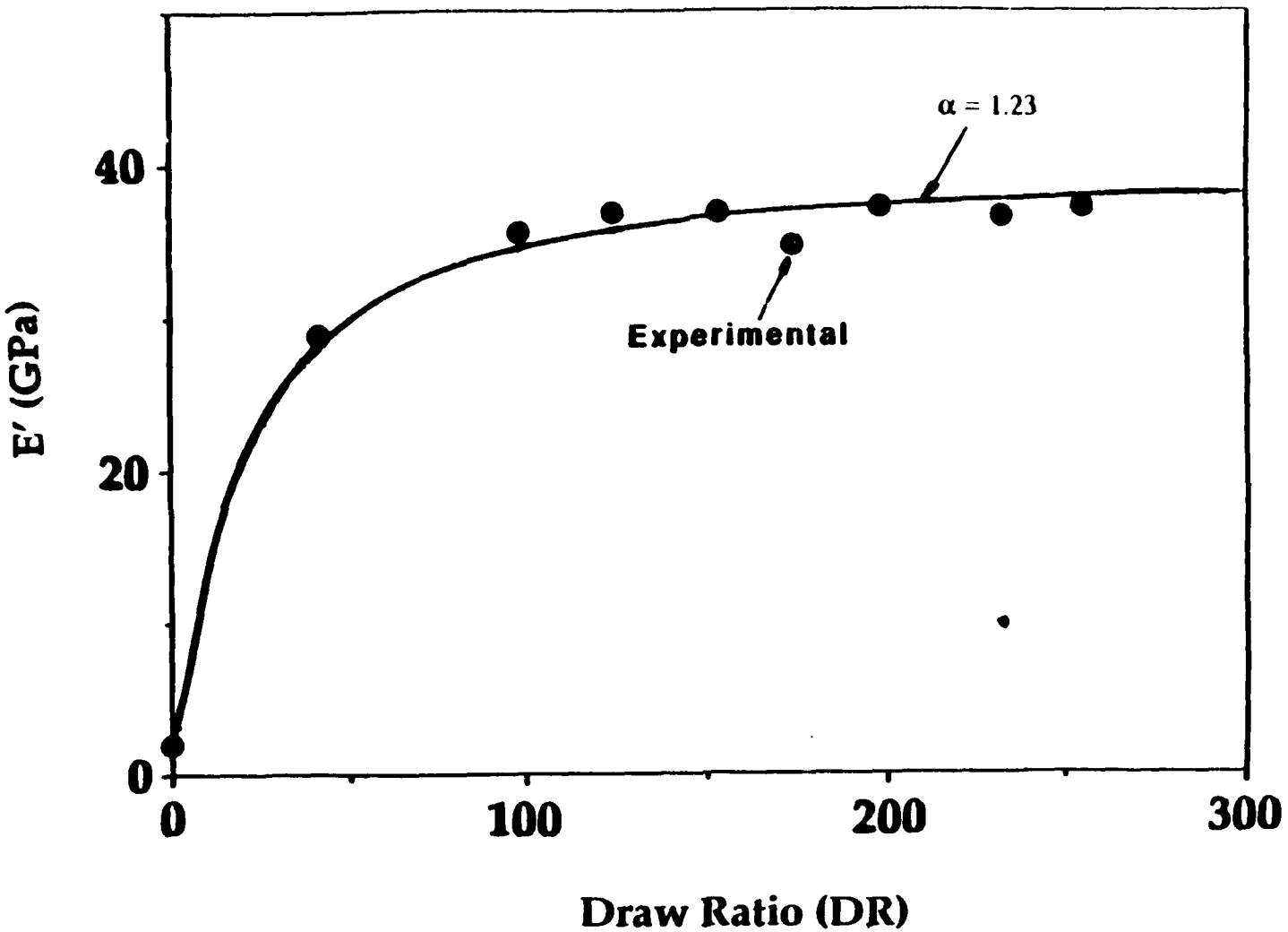

Fig. 3 Modulus data of PET/PHB60[25] fitted with the model with $\alpha = 1.23$.

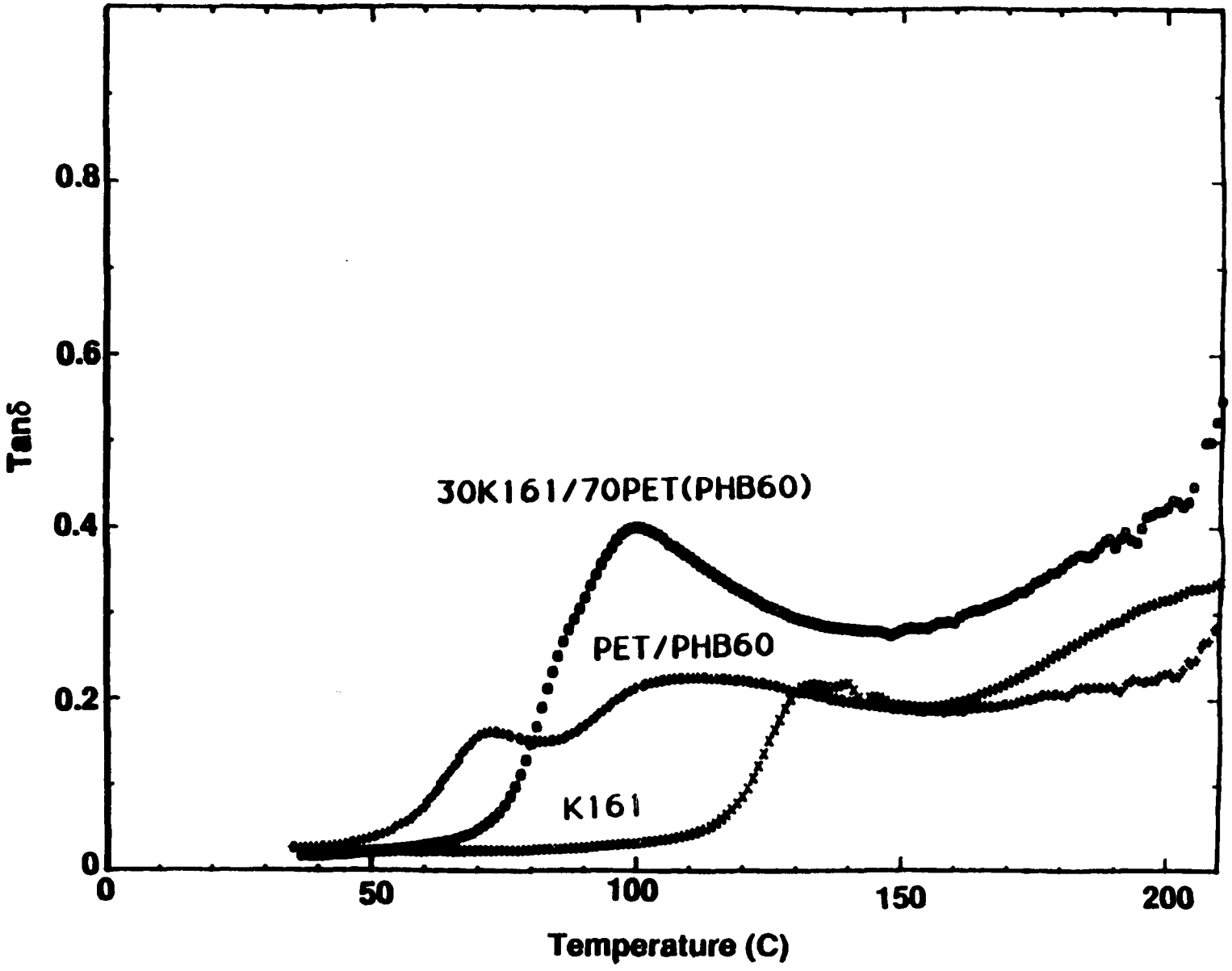

Fig. 4 Comparison of loss tangent, tan δ, for K161, PET/PHB60 and the blend of the two with 30/70 wt. ratio.

Fig. 5 30K161/70PET(PHB60) mixture annealed for (a) 0 hr. (b) 4 hrs. (c) 8 hrs.

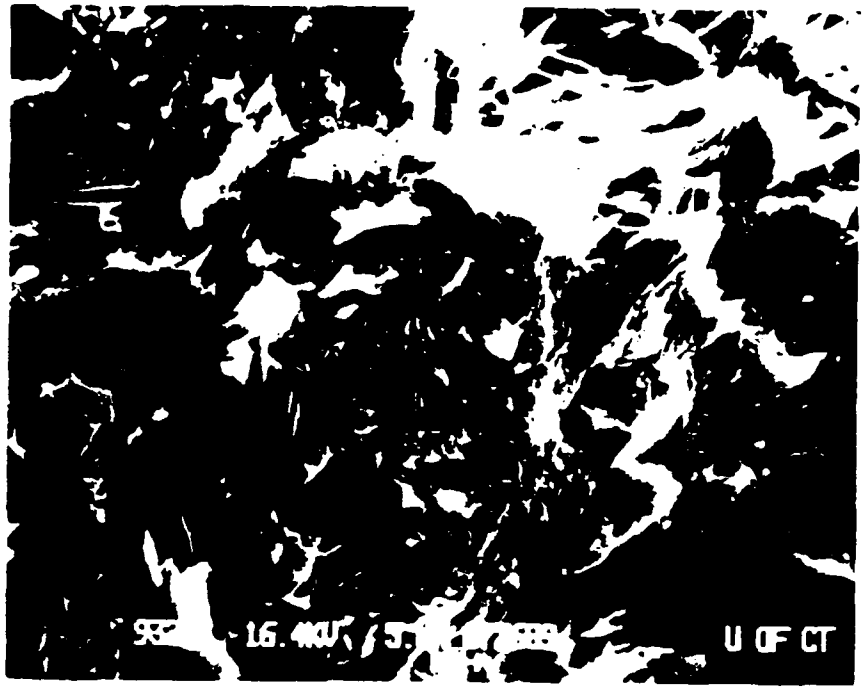

(a)

Fig. 5 30K161/70PET(PHB60) mixture annealed for (a) 0 hr. (b) 4 hrs. (c) 8 hrs.

(b)

(Continued from the previous page.)

Fig. 5 30K161/70PET(PHB60) mixture annealed for (a) 0 hr. (b) 4 hrs. (c) 8 hrs.

(c)

(Continued from the previous page.)

Fig. 6 Close-ups of the annealed samples for (a) 4 hrs. (b) 24 hrs.

(a)

Fig. 6 Close-ups of the annealed samples for (a) 4 hrs. (b) 24 hrs.

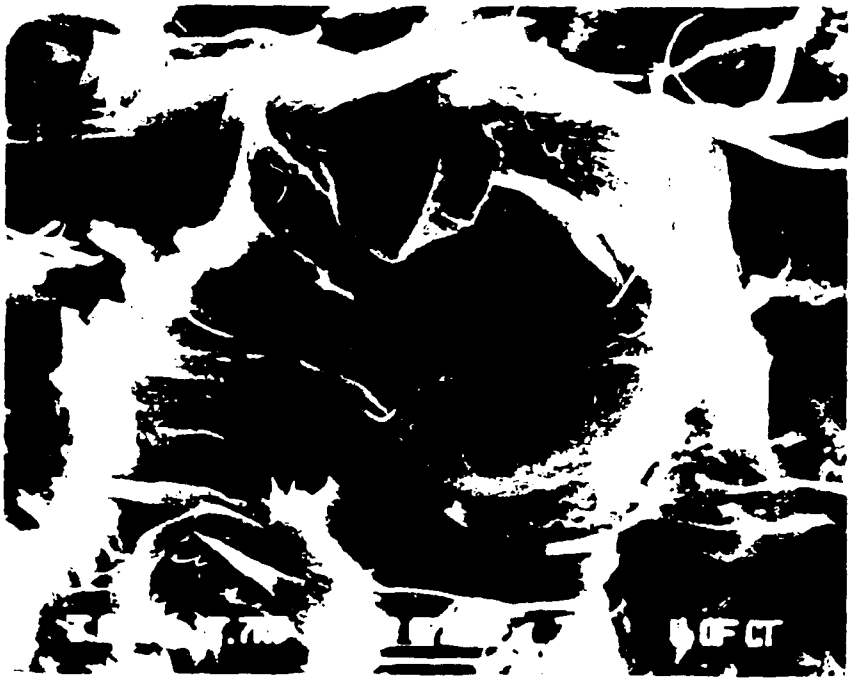

(b)

(Continued from the previous page.)

Fig. 7 Facture surface of the fiber obtain from 30K161/70PET(PHB60) blend.

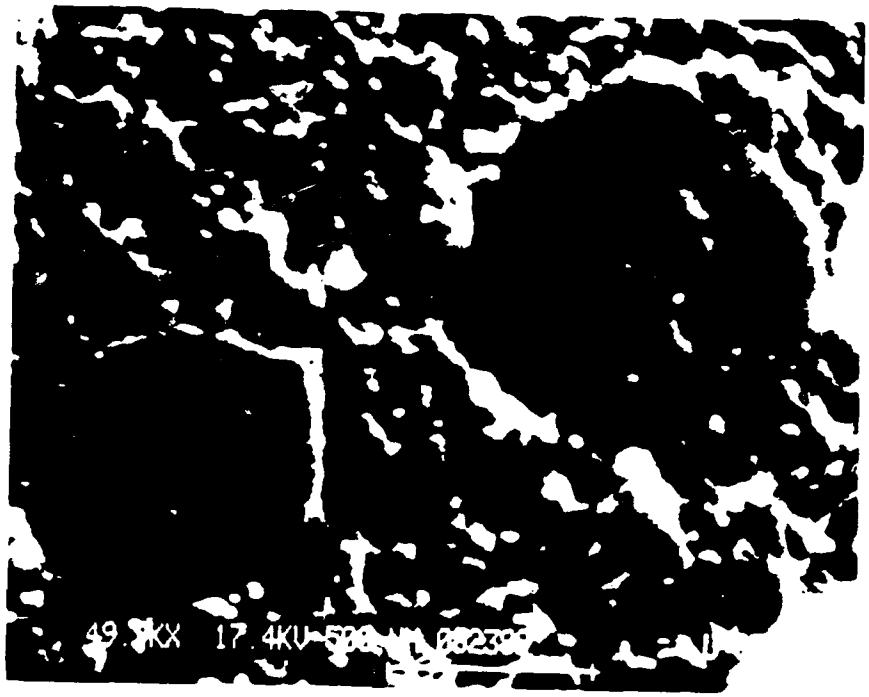

Fig. 8 Longitudinal fracture surface of the fiber from 30K161/70PET(PHB60) blend. (a) overall view of the broken fiber (b) close-up of the bundle, and (c) fibrils (~ 50*nm*) of PET/PHB60-rich phase

(a)

Fig. 8 Longitudinal fracture surface of the fiber from 30K161/70PET(PHB60) blend. (a) overall view of the broken fiber (b) close-up of the bundle, and (c) fibrils (~ 50*nm*) of PET/PHB60-rich phase

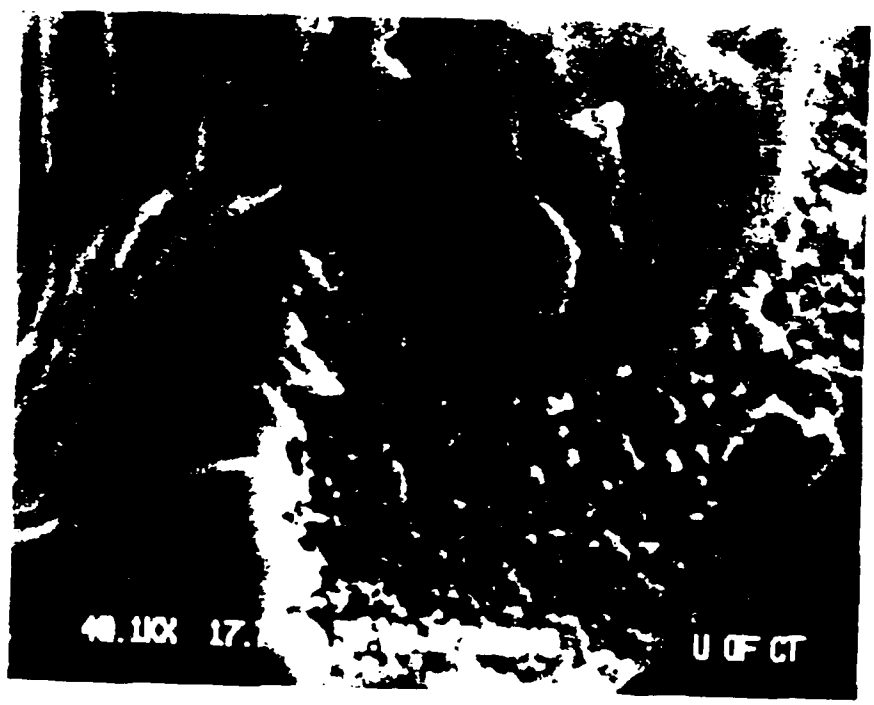

(b)

(Continued from the previous page.)

Fig. 8 Longitudinal fracture surface of the fiber from 30K161/70PET(PHB60) blend. (a) overall view of the broken fiber (b) close-up of the bundle, and (c) fibrils (~ 50*nm*) of PET/PHB60-rich phase

(c)

(Continued from the previous page.)

Fig. 9 TEM photographs of the fiber from 30K161/70PET(PHB60) blend. (a) & (b) are the transverse direction and (c) is the longitudinal direction.

(a)

Fig. 9 TEM photographs of the fiber from 30K161/70PET(PHB60) blend. (a) & (b) are the transverse direction and (c) is the longitudinal direction.

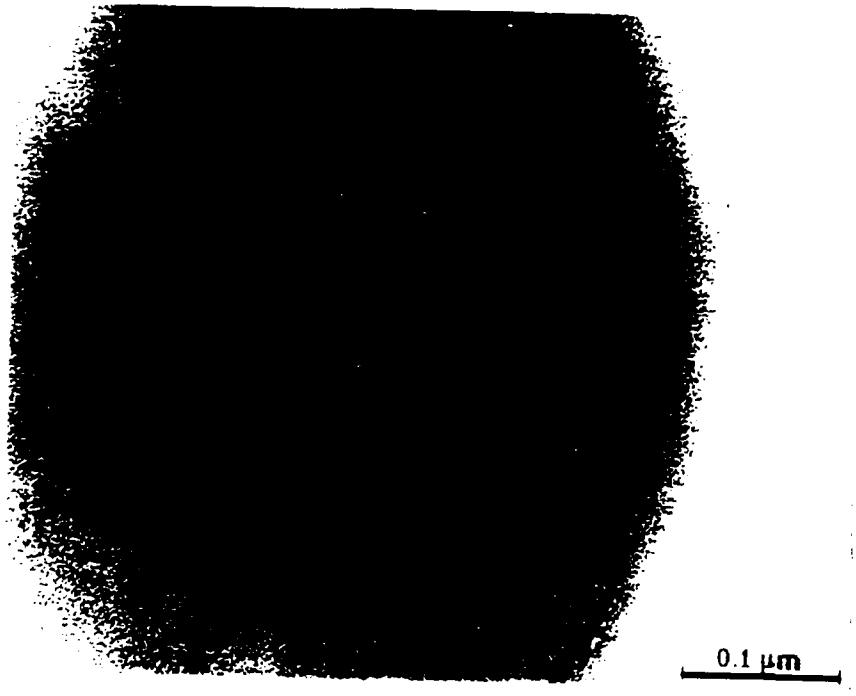

(b)

(Continued from the previous page.)

Fig. 9 TEM photographs of the fiber from 30K161/70PET(PHB60) blend. (a) & (b) are the transverse direction and (c) is the longitudinal direction.

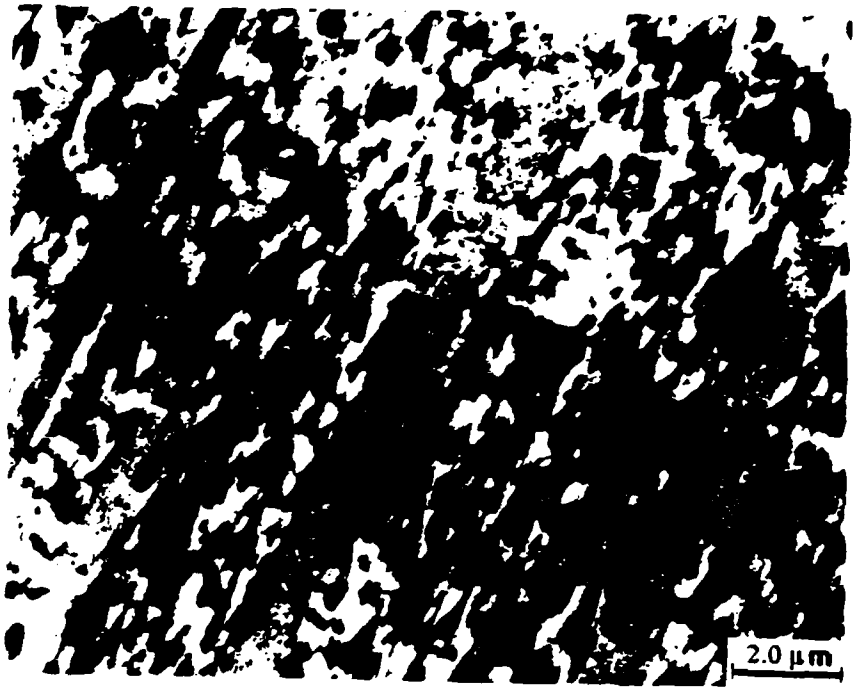

(c)

(Continued from the previous page.)

Materials	Breaking Strength (MPa)	Breaking strain (%)	Young's Modulus (GPa)
K161	332.65 ± 30.21	1.32 ± 0.07	28.47 ± 5.11
PET/PHB60	271.66 ± 38.94	1.81 ± 0.26	21.12 ± 2.69
30K161/70PET(PHB60)	242.09 ± 25.55	1.40 ± 0.28	25.11 ± 4.69
* Rule of Mixture	289.96 ± 36.32	—	23.33 ± 3.41

Table 1. Summary of the mechanical properties of LCP fibers.

TECHNICAL REPORT DISTRIBUTION LIST, GEN

	No. Copies
Office of Naval Research Attn: Code 1113 800 N. Quincy Street Arlington, Virginia 22217-5000	2
Dr. Bernard Douda Naval Weapons Support Center Code 50C Crane, Indiana 47522-5050	1
Naval Civil Engineering Laboratory Attn: Dr. R. W. Drisko, Code L52 Port Hueneme, California 93401	1
Defense Technical Information Center Building 5, Cameron Station Alexandria, Virginia 22314	12 high quality
DTNSRDC Attn: Dr. H. Singerman Applied Chemistry Division Annapolis, Maryland 21401	1
Dr. William Tolles Superintendent Chemistry Division, Code 6100 Naval Research Laboratory Washington, D.C. 20375-5000	1
Dr. David Young Code 334 NORDA NSTL, Mississippi 39529	1
Naval Weapons Center Attn: Dr. Ron Atkins Chemistry Division China Lake, California 93555	1
Scientific Advisor Commandant of the Marine Corps Code RD-1 Washington, D.C. 20380	1
U.S. Army Research Office Attn: CRD-AA-IP P.O. Box 12211 Research Triangle Park, NC 27709	1
Mr. John Boyle Materials Branch Naval Ship Engineering Center Philadelphia, Pennsylvania 19112	1
Naval Ocean Systems Center Attn: Dr. S. Yamamoto Marine Sciences Division San Diego, California 91232	1